Supplementary Materials

Table S1. OCA1 genetic changes, which affect the N-glycosylation sequence pattern

N-glycosylation site	N-glycosylation sequence pattern	OCA1 genetic changes which might affect the N-glycosylation pattern in putative positions:							
		-2	-1	0	+1	+2	+3	+4	+5
N86	84 FY**N**R**T**CCC 91	F84V					C89R	Q90R	C91S C91Y
N111	109 GP**N**C**T**ERR 116	G109R							
N161	159 MK**N**C**T**ERR 166								
N230	228 DE**N**F**T**IPY 235			**N230K**				P234T	Y235H
N290	288 LC**N**G**T**PEG 295	L288S L288F	C289R C289G C289Y					E294K E294G	G295R
N337	335 AA**N**F**S**FRT 342					**S339G**	F340L		
N371	369 YM**N**G**T**MSQ 376	Y369C	M370T M370I	**N371Y** **N371T**	G372R	**T373K**			

Seven sequons, N-X-T/S of human tyrosinase N-glycosylation are shown. X represents any amino acid except proline. The most severe mutations related to the position 0 (substitution of N) and +2 (substitution of S or T) are shown in red. In addition, according to Mazola et al., 2011 replacing of amino acids from positions -2 up to +5 could affect the glycosylation as well. OCA1 missense mutations, which potentially could affect the N-glycosylation were selected from the Human Gene Mutation Database (http://www.hgmd.cf.ac.uk/ac/all.php).

Figure S1. N-glycosylation of the human tyrosinase

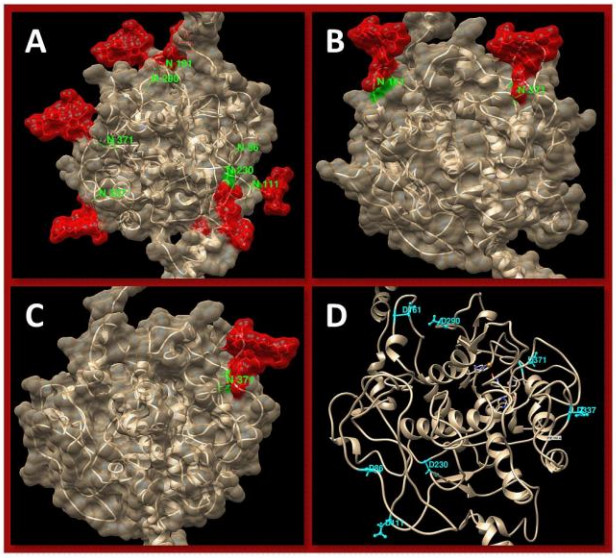

N-glycosylation site	5-deglycosylated mutant	6-deglycosylated mutant	7-deglycosylated mutant
N86	N86D	N86D	N86D
N111	N111D	N111D	N111D
N161	N161	N161D	N161D
N230	N230D	N230D	N230D
N290	N290D	N290D	N290D
N337	N337D	N337D	N337D
N371	N371	N371	N371D

The cartoon shows the proteins structure of N-glycosylated hTyrC$_{tr}$ (**A**) and 5-, 6-, and 7-deglycosylated mutant variants (5D (**B**), 6D (**C**), and 7D (**D**), respectively). All mutants were obtained from the tyrosinase intra-melanosomal domain using multiple site-directed mutagenesis. The protein backbone structures are depicted as a beige cartoon ribbons and the protein surfaces are shown as a beige mesh. Glycans are shown attached to their respective asparagine side chains as the red structures with the surfaces shown as a red mesh. The table shows numbered seven N-glycosylation sites of human tyrosinase and the multiple site-directed mutagenesis of 5, 6, and 7-deglycosylated mutant variants (5D, 6D, and 7D, respectively), in which the asparagine residues (N) were replaced with aspartic acids (D) to remove glycans in N-glycosylation sites and keep protein solubility by using of negatively charged residues instead. Residues shown in red were not changed in mutant variants.

Figure S2. Enzymatic deglycosylation of the recombinant hTyrC$_{tr}$ and 5 deglycosylated mutant variant (5D)

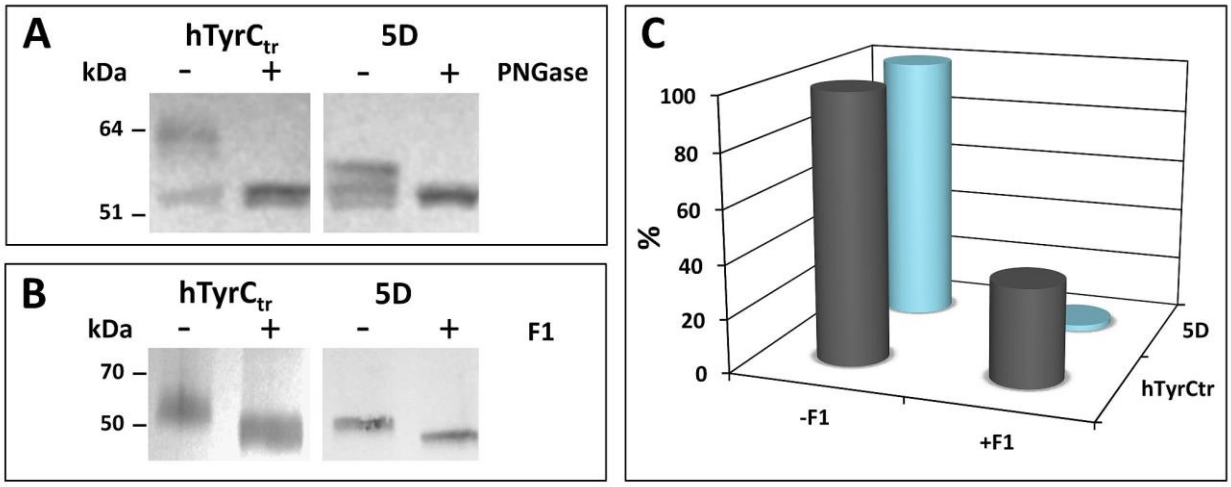

A: Deglycosylation of hTyrC$_{tr}$ (left panel) and 5-deglycosylated mutant variant (right panel) under denaturing conditions using PNGase F (N-Glycosidase F). Proteins were denatured in 50 mM sodium phosphate buffer, pH 7.5, using 0.2% SDS and 100 mM β-mercaptoethanol followed by heating at 100°C for 10 min. PNGase F (100 U) was then added and the mixtures were incubated at 37°C for 3 hours. Reactions were stopped by heating at 100°C for 5 min. **B:** Deglycosylation of hTyrC$_{tr}$ (left panel) and 5-deglycosylated mutant variant (right panel) under native condition using Endoglycosidase F1 (F1). Proteins were mixed with F1 solution in ratio 7:1 and incubated at 37°C for 1 hour. For both reactions, proteins analyzed by SDS-PAGE using 4–15% gradient gels and blotted using anti-tyrosinase T311 antibody (1:2000 dilution, Santa Cruz Biotechnology, Santa Cruz, CA, USA). **C:** Specific activity of pure hTyrC$_{tr}$ (grey bars) and 5-deglycosylated mutant variant (cyan bars) after the treatment in the presence (+F1) or in the absence (-F1) of Endoglycosidase F1 is shown as a percent of non-deglycosylated protein assuming 100% of activity for intact proteins.

Figure S3. SEC and enzymatic activities for the recombinant hTyrC$_{tr}$ and deglycosylated mutant variants

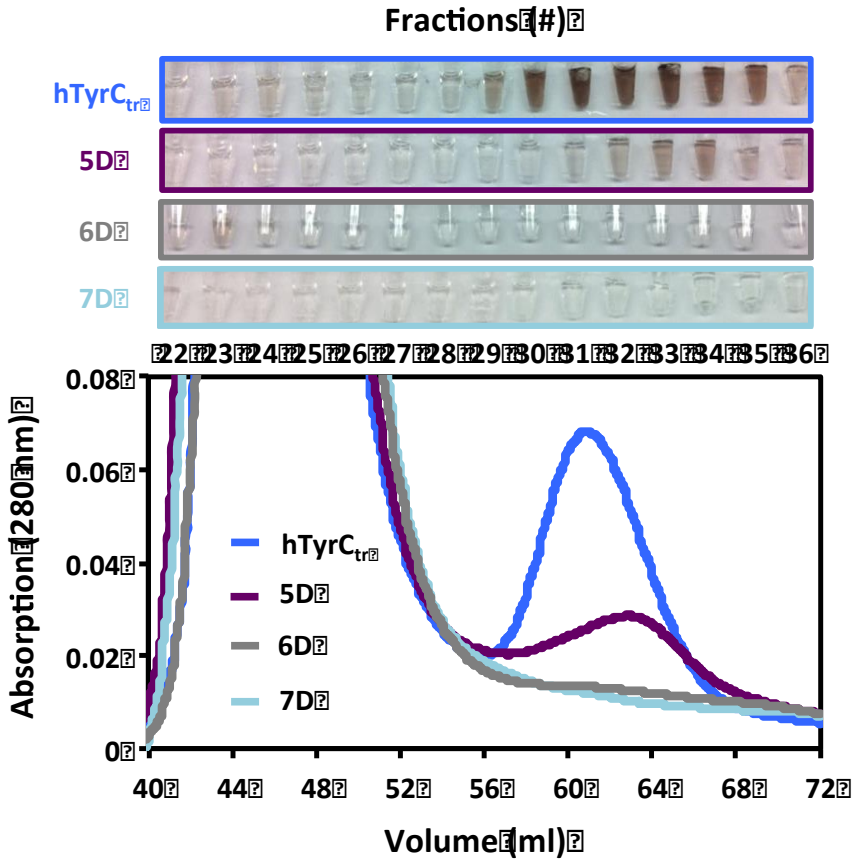

Recombinant tyrosinases (hTyrC$_{tr}$, blue; 5D, purple; 6D, grey; 7D, cyan, bottom panel) were eluted from 120 ml Superdex 75 16/60 column (GE Healthcare, Piscataway, NJ, USA) at a flow rate of 0.5 ml/min using a Bio-Logic Duo-Flow Maximizer workstation (Bio-Rad, Hercules, CA, USA). 2.5 ml fractions were collected. Brown color (intensity proportional) in tubes (top panels) indicates diphenol oxidase activity, measured for each fraction after 30 min of incubation at 37°C with 3 mM L-DOPA in 50 mM sodium phosphate buffer, pH 7.5. Protein fractions for the 6D mutant variant barely show color reaction in this experiment due to low protein

concentration. However, the 6D mutant have shown a recognizable enzymatic activity after protein concentration (data not shown).

Figure S4. Protein purity of recombinant hTyrC$_{tr}$ and deglycosylated mutant variants

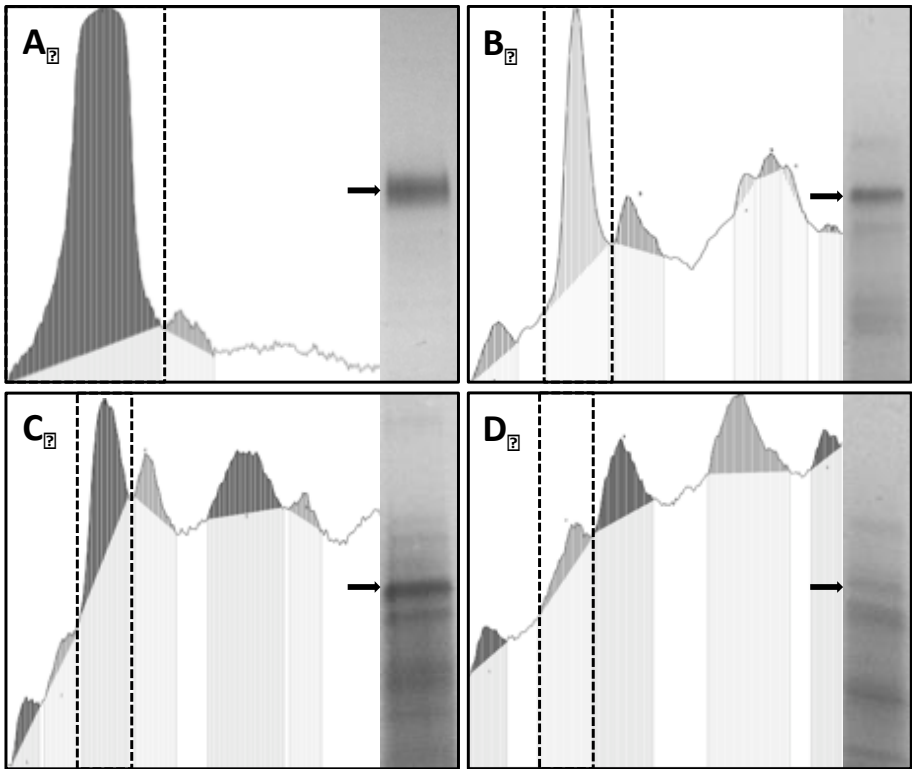

Protein purity of hTyrC$_{tr}$ (**A**), 5-deglycosylated mutant variant (5D) (**B**), 6-deglycosylated mutant variant (6D) (**C**), and 7-deglycosylated mutant variant (7D) (**D**) was obtained after three steps of chromatography from the SDS-PAGE gels (vertical inserts) using the UN-SCAN-IT gel ^{TM} analysis software (Silk Scientific, Inc., Orem, UT, USA). Areas of peaks in dotted rectangles is proportional to tyrosinase quantity and estimated to be 97.71, 73.54, 46.06, and 13.47%, respectively. Arrows indicate the tyrosinase bands with polypeptide molecular weight of ~65 kDa obtained using 4-20% gradient SDS-PAGE gel (Bio-Rad, Hercules, CA, USA).

Figure S5. Protein stability changes for deglycosylated mutant variants estimated from a link between tyrosinase conformational stability and enzymatic activity for OCA1B missense mutations

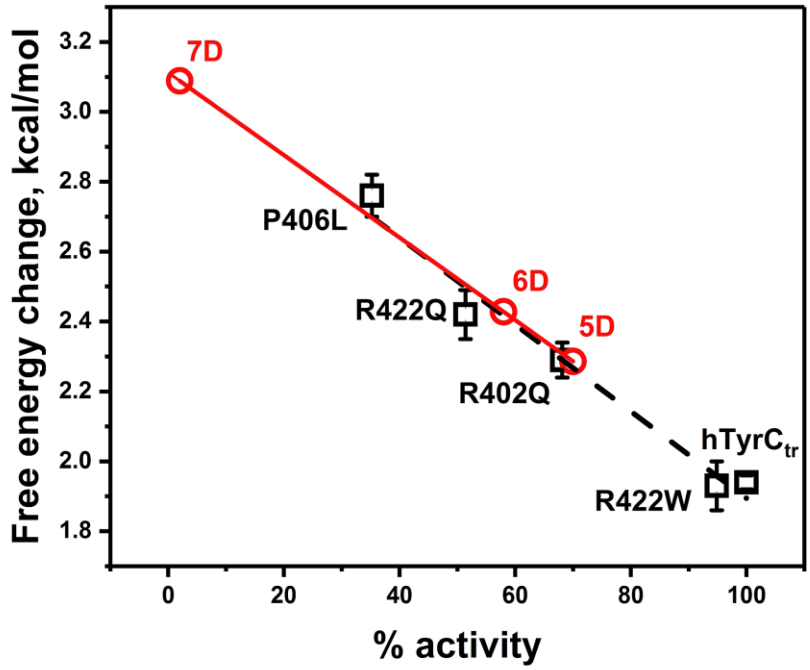

Gibbs free energy changes, ΔG, for OCA1B missense mutant variants were obtained from Dolinska et al, 2017. The changes are shown by black open squares with error bars. A linear equation demonstrating a link between protein stability and relative mutant protein activity (black dashed line) was obtained from fitting to experimental free energies, ΔG = 3.11208 - 0.0118 * (% activity). Protein stabilities for deglycosylated mutant variants (5D, 6D, and 7D) were estimated from this equation using relative specific activities from the Table 1 (open red circles) and were fitted using a red line.